Research Paper
Computational Methods for Differential Equations
http://cmde.tabrizu.ac.ir
Vol. *, No. *, *, pp. 1-8
DOI:10.22034/cmde.2026.74116.3821

A mathematical study for an air pollution model: stability, convergence and numerical verification

Karim Ivaz[1,*] , Ghader Darkhoshi[1], Sina Ivaz[2], and Mehran Paziresh[1]

[1]Department of Applied Mathematics, Faculty of Mathematics, Statistics and Computer Science, University of Tabriz, Tabriz 5166616471, East Azerbaijan, Iran.

[2]Graduate of Biomedical Engineering from Tabriz University of Technology (Sahand), Tabriz, Iran.

Abstract

This work presents the development and numerical analysis of a computational approach for solving an air pollution model formulated as a free-boundary problem. The numerical scheme employs the Variable Space Grid technique in conjunction with an explicit finite-difference discretization for the one-dimensional one-phase formulation. The obtained numerical results demonstrate strong agreement with the corresponding exact solutions and exhibit the anticipated convergence behavior as the spatial grid is progressively refined.

Keywords. Free boundary problem, Variable Space Grid (VSG) method, advection-diffusion equation, Von Neumann stability analysis, pollutant dispersion, finite difference scheme.

2010 Mathematics Subject Classification. 35K55, 76E06, 65M08, 35R35.

1. Introduction

This study is concerned with the numerical treatment of a free-boundary problem that arises in the context of air pollution modeling [3]. The governing system is given by

$$\frac{\partial c}{\partial t} + v\frac{\partial c}{\partial x} = \frac{\partial^2 c}{\partial x^2} + s(x,t), \qquad 0 < t < T, \;\; 0 < x < \psi(t), \tag{1.1}$$
$$c(x,0) = h(x), \tag{1.2}$$
$$c(\psi(t),t) = 0, \qquad 0 < t < T, \tag{1.3}$$
$$c(0,t) = g(t) \qquad 0 < t < T, \tag{1.4}$$
$$\psi(0) = b > 0, \tag{1.5}$$
$$c_x(\psi(t),t) = -\psi'(t), \qquad 0 < t < T. \tag{1.6}$$

In this system, the function $c(x,t)$ represents the concentration of a pollutant at spatial coordinate x and time t. The parameter v denotes the wind speed, while D represents the diffusion coefficient, and $s(x,t)$ accounts for the emission source. The unknown curve $x = \psi(t)$ defines the moving interface that separates the contaminated domain from the clean one. The initial concentration profile $h(x)$ is assumed to have compact support and satisfies $0 \leq h \leq M$. Furthermore, the source term and boundary functions are supposed to fulfill the required regularity assumptions. The well-posedness of the solution pair $(c(x,t), \phi(t))$ to (1.1)–(1.6) has been rigorously proved in [6] by means of the Friedman–Rubinstein integral representation combined with Banach's fixed-point theorem. In particular, it was shown

Received: 13 August 2026; Accepted: 10 September 2026.
∗ Corresponding author. Email: ivaz@tabrizu.ac.ir.

that, provided h, g, and s are continuously differentiable, the system (1.1)–(1.6) possesses a unique solution for all finite times, and the concentration satisfies

$$0 \le c(x,t) \le M, \quad c(\cdot,t) \text{ has bounded support.} \tag{1.7}$$

When the data possess additional smoothness, the solution inherits improved regularity. More precisely, if h and g are of class C^1 and s is sufficiently regular, then $c(\cdot,t)$ becomes continuously differentiable and the free boundary $\psi(t)$ is differentiable with respect to time [6].

Air pollution continues to pose a serious environmental threat, especially in densely populated and industrial regions where human activities and weather conditions aggravate the accumulation of contaminants. Key contributing factors include urban sprawl, industrial production, traffic emissions, and regional wind patterns, all of which significantly degrade air quality and endanger both human health and ecosystem stability [8–10]. Consequently, a thorough understanding and reliable forecasting of pollutant dispersion are crucial for devising effective control policies and enhancing environmental protection.

Owing to the inherently time-dependent nature of atmospheric pollutant transport, the boundaries of the affected zone are not stationary but shift continuously. In this work, we present a free-boundary formulation for an air pollution model, following the ideas introduced in [1, 4]. A broad spectrum of mathematical and numerical techniques has been developed for free-boundary problems, including those of Stefan type [2, 6, 7]. The free-boundary approach offers a notable benefit in that it allows the contamination front to evolve dynamically over time, thereby yielding more realistic predictions of pollutant spread under varying environmental conditions.

2. Numerical Method: Variable Space Grid (VSG) Approach

For the numerical solution of the one-dimensional free-boundary problem (1.1)–(1.6), we adopt the Variable Space Grid (VSG) technique, in which the total number of spatial subintervals N between the fixed boundary at $x = 0$ and the moving interface is kept fixed throughout the computation. Thus, the moving boundary always coincides with the N-th grid node. Let $x_i(t)$ denote the position of the i-th grid point. Differentiating $c(x_i(t), t)$ with respect to time yields [5]

$$\left.\frac{\partial c}{\partial t}\right|_{x_i} = \left.\frac{\partial c}{\partial x}\right|_{x_i} \frac{dx_i}{dt} + \left.\frac{\partial c}{\partial t}\right|_{x}.$$

Differentiating $c(x_i(t), t)$ with respect to time yields

$$\left.\frac{dc}{dt}\right|_{x_i(t)} = \left.\frac{\partial c}{\partial x}\right|_{x_i(t)} \frac{dx_i}{dt} + \left.\frac{\partial c}{\partial t}\right|_{x}.$$

Since $\frac{dx_i}{dt} = \frac{x_i}{\psi(t)}\psi'(t)$, after dropping subscripts for notational convenience, the original advection-diffusion equation (1.1) is rewritten as

$$\frac{\partial c}{\partial t} = \left(\frac{x_i}{\psi(t)}\psi'(t) - v\right)\frac{\partial c}{\partial x} + D\frac{\partial^2 c}{\partial x^2}. \tag{2.1}$$

Note that here $\frac{\partial c}{\partial t}$ on the left-hand side denotes the time rate of change of c following the moving node $x_i(t)$.

$$\frac{\partial c}{\partial t} = \left(\frac{x_i}{\psi(t)}\psi'(t) - v\right)\frac{\partial c}{\partial x} + D\frac{\partial^2 c}{\partial x^2}. \tag{2.1}$$

The grid spacing is defined by

$$\Delta x(t) = \frac{\psi(t)}{N}, \tag{2.2}$$

which varies over time as a consequence of the movement of the free boundary.

At the moving interface $x = \psi(t)$, the spatial derivative is approximated using a three-point backward difference scheme [2]:

$$\left.\frac{\partial c}{\partial x}\right|_{x=\psi(t)} = \frac{3c_N - 4c_{N-1} + c_{N-2}}{2\Delta x} + O(\Delta x^2). \tag{2.3}$$

An explicit finite-difference discretization of (2.1) is expressed as

$$C_i^{m+1} = C_i^m + \left(\frac{kx_i^m \Psi'_m}{h_m \Psi_m} - \frac{kv}{h_m}\right)\left(C_{i+1}^m - C_{i-1}^m\right) + \frac{kD}{h_m^2}\left(C_{i+1}^m - 2C_i^m + C_{i-1}^m\right), \tag{2.4}$$

where

$$C_i^m \approx c(x_i^m, t_m), \qquad \Psi_m \approx \psi(t_m) \quad x_i^m = ih_m, \qquad t_m = t_0 + mk, \qquad h_m = \frac{\psi(t_m)}{N}, \qquad k = \Delta t,$$

$$\Psi_0 = b, \Psi'_0 = 0,\ and\ \Psi'_m = \frac{\Psi_m - \Psi_{m-1}}{\Delta t},\ m \geq 1.$$

The boundary condition imposed at $x = 0$ becomes

$$C_0^m = g(t_m).$$

Consequently, the explicit scheme can be written as

$$C_i^{m+1} = C_i^m + \left(\frac{kx_i^m \Psi'_m}{h_m \Psi_m} - \frac{kv}{h_m}\right)(C_{i+1}^m - C_{i-1}^m) + \frac{kD}{h_m^2}(C_{i+1}^m - 2C_i^m + C_{i-1}^m), \tag{2.5}$$

for $i = 1, \ldots, N-1$, $m = 0, 1, 2, \ldots$, with $C_N^m = 0$.

The update rule for the free boundary is derived from (2.3):

$$\Psi_{m+1} = \Psi_m + \frac{k}{2h_m}\left(3C_N^m - 4C_{N-1}^m + C_{N-2}^m\right), \qquad \Psi_0 = b. \tag{2.6}$$

The grid spacing is then updated accordingly:

$$h_{m+1} = \frac{\psi_{m+1}}{N}. \tag{2.7}$$

The well-posedness of the continuous problem (1.1)–(1.6) is guaranteed by the theoretical findings reported in [3]. In the subsequent section, we analyze the convergence and stability properties of the numerical scheme defined by (2.5)–(2.6).

3. Convergence and Stability

A fundamental aspect of any numerical method is the proof of its convergence. Accordingly, we begin by examining the convergence of the scheme proposed in this work. By selecting the grid points as $C_{j,m} = c_{j,m} - e_j^m$ and applying Taylor expansions, we derive from (2.5) the following expression:

$$\begin{aligned} e_j^{m+1} &= e_j^m + \left(\frac{kx_j^m \psi'_m}{2h\psi_m} - \frac{kv}{2h}\right)\left(e_{j+1}^m - e_{j-1}^m\right) + r\left(e_{j+1}^m - 2e_j^m + e_{j-1}^m\right) + ke_0^m s(x_j, t_m) \\ &+ k\Big[\left(\frac{\partial c}{\partial t}\right)(x_j, t_m + \Theta_1 k) - \left(\frac{\partial^2 c}{\partial x^2}\right)(x_j + \Theta_2 h, t_m) - \left(\frac{kx_j^m \psi'_m}{2h\psi_m} - \frac{kv}{2h}\right)\left(\frac{\partial c}{\partial x}\right)(x_i + \Theta_3 h, t_m) - s(x_j, t_m)\Big], \end{aligned}$$

which can be rearranged as

$$\begin{aligned} e_j^{m+1} &= (1-2r)e_j^m + \left(r + \frac{kx_j^m \psi'_m}{2h\psi_m} - \frac{kv}{2h}\right)\left(e_{j+1}^m - e_{j-1}^m\right) + ke_0^m s(x_j, t_m) \\ &+ k\Big[\left(\frac{\partial c}{\partial t}\right)(x_j, t_m + \Theta_1 k) - \left(\frac{\partial^2 c}{\partial x^2}\right)(x_j + \Theta_2 h, t_m) - \left(\frac{kx_j^m \psi'_m}{2h\psi_m} - \frac{kv}{2h}\right)\left(\frac{\partial c}{\partial x}\right)(x_j + \Theta_3 h, t_m) + s(x_j, t_m)\Big] \end{aligned} \tag{3.1}$$

where $r = \dfrac{k}{h^2}$ and the constants satisfy $-1 < \Theta_2 < 1$, $0 < \Theta_1, \Theta_3 < 1$. Provided that the time step satisfies the condition $k < \frac{h^2}{2}$ and $h < \dfrac{2\psi_m}{v\psi_m - x_j^m \psi_m'}$ for each step with indices $h, k, j = 1, \dots, N-1$ and $m = 0, 1, \dots$, we may write

$$e_j^{m+1} \leq (1-2r)|e_j^m| + \Big(r + \frac{kx_j^m\psi_m'}{2h\psi_m} - \frac{kv}{2h}\Big)|e_{j+1}^m| + \Big(r + \frac{kx_j^m\psi_m'}{2h\psi_m} - \frac{kv}{2h}\Big)|e_{j-1}^m| + kM_1 + kN_1. \tag{3.2}$$

Let ER^m denote the maximum absolute error $|e_j^m|$ over the entire spatial grid at the m-th time level. Furthermore, let M_1 represent the maximum value of the bracketed terms in (3.2) over all indices j and m, and let N_1 be the maximum of $|e_0^m s(x_j, t_m)|$. Consequently, we obtain

$$\begin{aligned} ER^{m+1} &\leq ER^m + kM_1 + kN_1 \\ &\leq ER^{m-1} + kM_1 + kM_1 + kN_1 \\ &= ER^{m-1} + 2k(M_1 + N_1) \\ &\leq \ldots \leq ER^0 + mk(M_1 + N_1). \end{aligned} \tag{3.3}$$

From (3.3), it follows that $ER^m \leq ER^0 + mk(M_1 + N_1)$. Since the initial values of c and C coincide, we have $ER^0 = 0$. In the limit $h \to 0$ with $k = rh^2$, the quantity M_1 tends to

$$\Big[\Big(\frac{\partial c}{\partial t}\Big) - \Big(\frac{\partial^2 c}{\partial x^2}\Big) - \Big(\frac{kx_j^m\psi_m'}{2h\psi_m} - \frac{kv}{2h}\Big)\Big(\frac{\partial c}{\partial x}\Big)\Big]_j^m.$$

Given that c, ψ, and M_1 are bounded, we conclude that $ER^m = 0$.

From the bound $|C_j^m - c_i^m| \leq ER^m$ for $m = 0, 1, \dots$, it follows that under the condition $k < \frac{2h^2}{4 + h(\psi_m' - v)}$ for all m, as $h \to 0$, the numerical solution C converges to the exact solution c.

To establish the convergence of Ψ_m to ψ_m, we employ the update relation (2.6) and introduce the representations $\Psi_{m+1} = \psi_{m+1} - e'_{m+1}$ and $\psi_m = \phi_m - e'_m$. This yields

$$\psi_{m+1} - e'_{m+1} = \psi_m - e'_m - \frac{k}{2h}\Big(3C_N^m - 3e_N^m - 4C_{N-1}^m + 4e_{N-1}^m + C_{N-2}^m - e_{N-2}^m\Big),$$

and therefore

$$e'_{m+1} = e'_m + \psi_{m+1} - \psi_m + \frac{k}{2h}\Big(3c_N^m - 3e_N^m - 4c_{N-1}^m + 4e_{N-1}^m + c_{N-2}^m - e_{N-2}^m\Big).$$

By expanding the terms using Taylor series, we obtain

$$\begin{aligned} e'_{m+1} &= e'_m + k\psi'(t^m + \Theta_5 k) - \frac{3k}{2h}e_N^m + \frac{k}{2h}e_{N-1}^m - \frac{k}{2h}e_{N-2}^m \\ &\quad + \frac{k}{2h}\Big(3c_N^m - 4c_N^m + 4h\Big(\frac{\partial c}{\partial x}\Big)(x_N - \Theta_6 h, t^m) + c_N^m - 2h\Big(\frac{\partial c}{\partial x}\Big)(x_N - \Theta_7 h, t^m)\Big), \end{aligned} \tag{3.4}$$

In (3.4), since $0 < \Theta_6 h, \Theta_7 h < h$, for sufficiently small step sizes h we have $\Theta_6 \approx \Theta_7$, which allows us to simplify the expression as

$$e'_{m+1} = e'_m + k\Big[\psi'(t^m + \Theta_5 k) + \Big(\frac{\partial c}{\partial x}\Big)(x_N - \Theta_6 h, t^m)\Big] - \frac{3k}{2h}e_N^m + \frac{k}{2h}e_{N-1}^m - \frac{k}{2h}e_{N-2}^m.$$

Consequently, taking absolute values leads to

$$|e'_{m+1}| \leq |e'_m| + k\Big|\Big[\psi'(t^m + \Theta_5 k) + \Big(\frac{\partial c}{\partial x}\Big)(x_N - \Theta_6 h, t^m)\Big]\Big| + \frac{3k}{2h}|e_N^m| + \frac{k}{2h}|e_{N-1}^m| + \frac{k}{2h}|e_{N-2}^m|. \tag{3.5}$$

Let $\prod$ denote the maximum value of the bracketed expression in (3.5). Then we have

$$\begin{aligned}|e'_{m+1}| &\le |e'_m| + k\prod + \Big(\frac{3k}{2h}+\frac{k}{2h}+\frac{k}{2h}\Big)E_m = |e'_m| + k\prod + \frac{4k}{h}E_m\\ &\le |e'_{m-1}| + 2k\prod + \frac{4k}{h}E_{m-1}\\ &\le \ldots \le |e'_0| + mk\prod + \frac{4k}{h}ER_0.\end{aligned}$$

Since the initial data for (ψ, c) and (Ψ, C) are identical, we have $e'_0 = 0$ and $ER_0 = 0$. As $k \to 0$, the quantity $\prod$ approaches $\Big(\psi' + \frac{\partial c}{\partial x}\big|_{x=\phi(t)}\Big)_m$. Because (ψ, c) is a solution of the original problem (1.1)-(1.6), in the joint limit $h \to 0$ and $k \to 0$, we obtain $\prod \to 0$, and hence $|e'_{m+1}| \to 0$. This confirms that Ψ converges to ψ.

3.1. **Stability.** We now examine the stability of the difference equation (3.6) for the case $F(v) = v$ using the von Neumann approach. The difference equation under consideration is

$$\zeta_j^{m+1} = \zeta_j^m + \Big(\frac{rh}{2\psi_m}\xi_j\psi'_m - \frac{kv}{2h}\Big)\Big(\zeta_{j+1}^m - \zeta_{j-1}^m\Big) + r\Big(\zeta_{j+1}^m - 2\zeta_j^m + \zeta_{j-1}^m\Big), \quad j = 1, \ldots, N-1, \quad m = 0, 1, 2, \ldots. \tag{3.6}$$

By substituting the Fourier mode $\zeta_j^m = A^m e^{i\theta j}$, with $i^2 = -1$, into the difference equation (3.6), we obtain

$$\begin{aligned}A^{m+1}e^{i\theta(j+1)} &= A^m e^{i\theta j} + \Big(\frac{rh}{2\psi_m}\xi_j\psi'_m - \frac{kv}{2h}\Big)\Big(A^m e^{i\theta(j+1)} - A^m e^{i\theta(j-1)}\Big)\\ &\quad + r\Big(A^m e^{i\theta(j+1)} - 2A^m e^{i\theta j} + A^m e^{i\theta(j-1)}\Big).\end{aligned} \tag{3.7}$$

This leads to

$$A^{m+1} = A^m + \Big(\frac{rh}{2\psi_m}\xi_j^m\psi'_m - \frac{kv}{2h}\Big)\Big(A^m e^{i\theta} - A^m e^{-i\theta}\Big) + r\Big(A^m e^{i\theta} - 2A^m + A^m e^{-i\theta}\Big),$$

which can be rewritten as

$$\begin{aligned}A &= \Big\{\ 1 + \Big(\frac{k}{2h\psi_m}\xi_j^m\psi'_m - \frac{kv}{2h}\Big)(e^{i\theta} - e^{-i\theta}) + r(e^{i\theta} - 2 + e^{-i\theta})\Big\}\\ &= \Big\{\ 1 - 2r + \Big[\frac{k}{2h\psi_m}\xi_j^m\psi'_m - \frac{kv}{2h}\Big](e^{i\theta} - e^{-i\theta}) + r(e^{i\theta} + e^{-i\theta})\Big\}\\ &= \Big\{\ 1 - 2r + 2r\cos\theta + i\Big[\frac{k}{h\psi_m}\xi_j^m\psi'_m - \frac{kv}{h}\Big]\sin\theta\Big\}\\ &= \Big\{\ 1 - 2r(1-\cos\theta) + i\Big[\frac{rh}{\psi_m}\xi_j^m\psi'_m - \frac{kv}{h}\Big]\sin\theta\Big\},\end{aligned} \tag{3.8}$$

Consequently, the modulus of A is given by

$$\begin{aligned}|A| &= \Big(1 - 2r(1-\cos\theta)\Big)^2 + \Big[\frac{k}{h\psi_m}\xi_j^m\psi'_m - \frac{kv}{h}\Big]^2\sin^2\theta\\ &= \Big(1 - 4r\sin^2\frac{\theta}{2}\Big)^2 + \Big[\frac{k}{h\psi_m}\xi_j^m\psi'_m - \frac{kv}{h}\Big]^2\sin^2\theta,\\ &= \Big(1 - 4r\sin^2\frac{\theta}{2}\Big)^2 + \Big[\frac{kj}{hN}\psi'_m - \frac{kv}{h}\Big]^2\sin^2\theta,\\ &= \Big(1 - 4r\sin^2\frac{\theta}{2}\Big)^2 + \frac{k^2}{h^2}\Big(\frac{j}{N}\psi'_m - v\Big)^2\sin^2\theta,\end{aligned} \tag{3.9}$$

We now establish that the von Neumann stability condition is satisfied for $|A|$ provided that $k \le \frac{2}{\beta}$, where $\beta = \Big(\frac{j}{N}\psi'_m - v\Big)^2$. Under this condition, we may write $k < \frac{2}{\frac{4}{h^2}+\beta-\frac{4}{h^2}}$, or equivalently $k\Big(\frac{4}{h^2} + \beta - \frac{4}{h^2}\Big) < 2$. For all values of θ, it follows that

$$|A| = \Big(1 - 4r\sin^2\frac{\theta}{2}\Big)^2 + \frac{k^2}{h^2}\Big(\frac{j}{N}\psi'_m - v\Big)^2 \sin^2\theta < 1.$$

4. Numerical Results

In this section, we present two test examples to demonstrate the accuracy of the proposed numerical scheme in comparison with the corresponding exact solutions.

Example 4.1. Consider the following one-phase free-boundary problem modeling air pollution:

$$\begin{aligned}
&\frac{\partial c}{\partial t} + v\frac{\partial c}{\partial x} = D\frac{\partial^2 c}{\partial x^2}, \quad t>0, \quad 0<x<\phi(t),\\
&c(0,t) = t, \quad t>0,\\
&c(x,0) = \frac{-x}{v}, \ \ v>0,\\
&c(\phi(t),t) = 0,\\
&-v^2 c_x(\phi(t),t) = \frac{d\phi}{dt}, \quad t>0, \quad 0<x<\phi(t),\\
&\phi(0) = 0.
\end{aligned} \tag{4.1}$$

The associated exact solution is given by

$$c(x,t) = \frac{1}{2\sqrt{D\pi t}}\left[\exp\left(-\frac{(vt-x)^2}{4Dt}\right) - \exp\left(\frac{vx}{D}\right)\exp\left(-\frac{(vt+x)^2}{4Dt}\right)\right] - \frac{x}{v} + t, \quad \phi(t) = vt,$$

where v denotes the wind speed (or convection velocity) and D represents the adhesion and permeability coefficient of the contaminated medium.

Figure 1 is generated using the following parameter values:

$$h = 10^{-2}, \ \ k = 10^{-6}, \ \ v = 1, \ \ 0.17 \le t \le 1, \ \ D = 1, \ \ \text{error} = 10^{-5}.$$

Table 1. Variable space grid: Values of the temperature distribution as predicted by the numerical (explicit finite-difference) and exact solutions at a final time of $t_f = 1$. N is the number of spatial subintervals, between the fixed boundary at $x = 0$ and the moving interface.

x/ϕ	$N = 10$	$N = 20$	$N = 40$	$N = 80$	Exact
0.0	1.7223	1.72	1.7194	1.7191	1.7191
0.1	1.4613	1.4602	1.4599	1.4598	1.4604
0.2	1.2257	1.2253	1.2253	1.2254	1.2263
0.3	1.013	1.0131	1.0133	1.0134	1.0145
0.4	0.82088	0.82125	0.82149	0.82163	0.82285
0.5	0.64736	0.64782	0.64808	0.64822	0.64941
0.6	0.49057	0.49101	0.49124	0.49138	0.49248
0.7	0.34887	0.34921	0.3494	0.3495	0.35047
0.8	0.22074	0.22097	0.22109	0.22116	0.22197
0.9	0.10486	0.10496	0.10502	0.10505	0.10569
1.0	0.0	0.0	0.0	0.0	0.0

Example 4.2. We now consider a free-boundary problem describing pollutant emission and transport, in which the source term exhibits negative growth:

$$
\begin{aligned}
&\frac{\partial c}{\partial t} + v\frac{\partial c}{\partial x} = \frac{\partial^2 c}{\partial x^2} - \frac{1}{v^2}e^{t-x}, \quad t>0, \quad 0<x<\phi(t),\\
&c(0,t) = e^t - 1, \quad t>0,\\
&c(x,0) = e^{\frac{-x}{v}} - 1, \;\; v>0,\\
&c(\phi(t),t) = 0,\\
&-v^2 c_x(\phi(t),t) = \frac{d\phi}{dt}, \quad t>0, \quad 0<x<\phi(t),\\
&\phi(0) = 0.
\end{aligned}
\tag{4.2}
$$

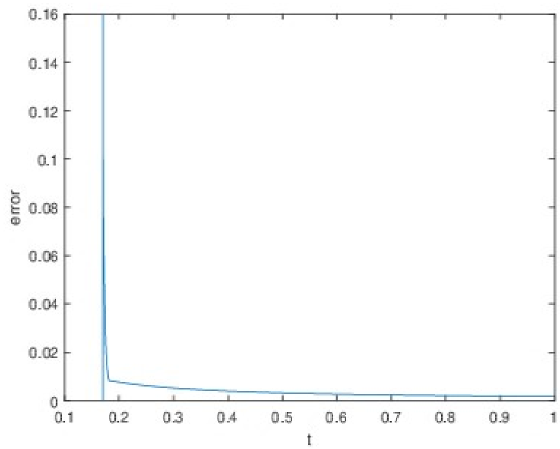

FIGURE 1. Error diagram of exact and approximate solution with accuracy of 10^{-3}.

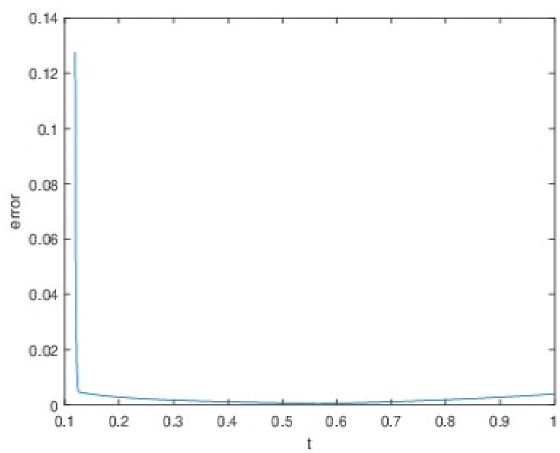

FIGURE 2. Error diagram of exact and approximate solution with accuracy of 10^{-4}.

This problem admits the following exact solution:

$$c(x,t) = \exp\left(t - \frac{x}{v}\right) - 1, \quad \phi(t) = vt.$$

Using the finite-difference scheme, Figure 2 displays the error between the exact and numerical solutions at the moving boundary.

Table 1 presents the numerical results for the concentration distribution and the interface position at the final time $t_f = 1$. The results are in excellent agreement with the exact solution, and the expected convergence behavior is observed as the spatial grid is refined. For instance, at $t_f = 0.5$, the percentage error decreases from $0.2 \times 10^{-2}\%$ when $N = 40$.

5. Conclusion

In this work, we have conducted a thorough investigation of a numerical approach applied to an air pollution model formulated as a one-phase free-boundary problem. The findings highlight the critical role of selecting an appropriate numerical technique for accurately simulating phase-change phenomena, which has significant implications for various fields, including materials science, cryogenics, and geophysics. Our results confirm the capability of the finite-difference method to effectively capture the dynamic evolution of the moving boundary that characterizes this class of air pollution models.

Acknowledgments

The authors would like to thank all colleagues and individuals who contributed to the completion of this work.

References

[1] D. Abdollahi, S. Ahdiaghdam, K. Ivaz, and R. Shabani, *A theoretical study for the vibration of a cantilever microbeam as a free boundary problem*, Appl. Math. Model. *40* (2016), 1836-1849.
[2] R. M. Furzeland, *A comparative study of numerical methods for moving boundary problems*, IMA Journal of Applied Mathematics *26*(4) (1980), 411-429.
[3] K. Ivaz and G. Darkhoshi, *A theoretical study for an air pollution model as a free boundary problem*, J. Math. Model. *14*(1) (2025), 115-135.
[4] K. Ivaz, D. Abdollahi, and R. Shabani, *Analyzing free vibration of a cantilever microbeam submerged in fluid with free boundary approach*, J. Appl. Fluid Mech. *10* (2017), 1593-1603.
[5] S. Kutluay, A. R. Bahadır, and A. Özdeş, *The numerical solution of one-phase classical Stefan problem*, J. Comput. Appl. Math. *81* (1997), 135-144.
[6] S. Sh. Pishnamaz Mohammad and K. Ivaz, *Numerical solution of one-phase Stefan problem for the non-classical heat equation with a convective condition*, Comput. Methods Differ. Equ. *14* (2023), 76-784.
[7] S. Sh. Pishnamaz Mohammad and K. Ivaz, *Numerical study of one-phase Stefan-type problems*, Iran. J. Math. Chem. *16* (2025), 27-139.
[8] J. H. Seinfeld and S. N. Pandis, *Atmospheric Chemistry and Physics: From Air Pollution to Climate Change*, John Wiley & Sons, Hoboken, 2016.
[9] A. Uma, S. Gakkhar, and R. S. Gupta, *Removal model suitable for air pollutants emitted from an elevated source*, Appl. Math. Model. *15* (1991), 386-389.
[10] S. D. Zawka and D. N. Srinivasu Pichika, *Existence and optimal harvesting of two competing species in a polluted environment with pollution reduction effect*, J. Math. Model. *9* (2021), 517-536.